Acta Cryst. (1976). B32, 1756

The Structure of $Ga_4Ti_{21}O_{48}$

BY D. J. LLOYD*

Chemistry Department, Monash University, Melbourne, Victoria, Australia

I. E. GREY

Division of Mineral Chemistry, CSIRO, P.O. Box 124, *Port Melbourne*, 3207, *Australia*

AND L. A. BURSILL

School of Physics, Melbourne University, Parkville, 3052, *Australia*

(*Received* 25 *August* 1975; *accepted* 17 *November* 1975)

Crystals of $Ga_4Ti_{21}O_{48}$ are monoclinic, space group $C2/m$, with $Z=2$, $a=51{\cdot}80$ (2), $b=2{\cdot}975$ (1), $c=10{\cdot}302$ (4) Å and $\beta=103{\cdot}80$ (2)°. Intensities for 1046 observed reflexions, collected on a four-circle diffractometer, were used in the structure solution which was refined to $R=0{\cdot}081$ and $wR=0{\cdot}096$. The structure is a coherent intergrowth, parallel to $(210)_r$, of rutile structure-type and elements similar to those in the β-gallia structure. Adjacent slabs of rutile structure-type are displaced by $[\frac{1}{2}\frac{1}{4}\frac{1}{2}]_r$. The structure may alternatively be described as a $[\frac{1}{2}\frac{1}{4}\frac{1}{2}]\,(210)_r$ crystallographic shear, *CS*, phase. Periodic application of this operation on $(210)_r$ planes produces an homologous series of *CS* phases of generic formula $Ga_4Ti_{m-4}O_{2m-2}$. In $Ga_4Ti_{21}O_{48}$ the gallium atoms are ordered into the *CS* planes. Within the *CS* planes, columns of β-Ga_2O_3 structure are separated by hexagonal tunnels, parallel to **b**, of mean effective diameter 2·5 Å. It has proved possible to directly image the tunnels in a high-resolution electron microscope.

Introduction

Gibb & Anderson (1972) reported the characterization of an homologous series of structures $Ga_4Ti_{m-4}O_{2m-2}$ ($15<m<23$, m odd) in the Ga_2O_3–TiO_2 system, using electron microscopy. Their electron diffraction contrast analysis suggested the structures were derived from the rutile structure-type by the periodic repetition of displacement boundaries parallel to the (210) planes of rutile. They deduced the displacement vector to be $[0\frac{1}{2}0]_r$ but were unable to derive a pure displacement boundary consistent with this vector. This is because $[0\frac{1}{2}0]_r$ is not an oxygen–oxygen vector, although it is a vector between filled and empty metal atom sites in rutile. Their proposed structure for the fault involved the shifting of the metal sites only by $[0\frac{1}{2}0]_r$† and leaving the anion sites unchanged. However the proposed structure (their Fig. 8) can alternatively be described by a pure displacement, $\frac{1}{2}[101]_r$ of *both* metals and anions and is therefore inconsistent with the observed diffraction contrast.

To resolve the problem we carried out a single-crystal X-ray structure analysis for one of the members of the homologous series, $Ga_4Ti_{21}O_{48}$. We found that the displacement vector at the $(210)_r$ boundaries is in fact $[\frac{1}{2}\frac{1}{4}\frac{1}{2}]_r$, a result which was obtained independently using an electron diffraction method (Bursill & Stone, 1975). The $(210)_r$ boundaries contain elements of the β-Ga_2O_3 structure (Geller, 1960) coherently intergrown with the rutile structure. The β-gallia elements are separated along the boundary by relatively large tunnels and it has proved possible to directly image the tunnels in a high-resolution electron microscope.

Experimental

The molar ratio $Ga_2O_3:10TiO_2$ was intimately ground, pelleted and heated for 16 hours at 1600 °C in oxygen, then cooled rapidly to room temperature. The reaction product was in the form of a light yellow, translucent, polycrystalline sinter with an average crystallite size of ~0·1 mm. A powder X-ray diffractogram showed a pattern very similar to that of rutile, Fig. 1, but with pronounced splitting of some lines, particularly the strongest $(110)_r$ line. A very small amount ($\lesssim 5\%$) of Ga_2TiO_5 was also evident in the diffractogram.

Weissenberg photographs on selected crystal fragments confirmed the observations of Gibb & Anderson (1972); *i.e.* a superstructure based on the rutile subcell with superlattice rows along g $(210)_r$. The Weissenberg photographs showed that crystals of a size suitable for an X-ray diffraction analysis always contained contributions from more than one superstructure. A crystal was finally selected which had a major diffraction contribution from a superstructure with 12 spots out to $(210)_r$; *i.e.* the homologue $Ga_4Ti_{21}O_{48}$, using Gibb & Anderson's formula. A second weak series of spots with intensities about one tenth of those from $Ga_4Ti_{21}O_{48}$ resulted from a minor amount of the adjacent homologue $Ga_4Ti_{19}O_{44}$.

* Present address: State College of Victoria, Bendigo, 3550, Australia.

† Subscript r indicates rutile-cell axes or indices.

The major component, $Ga_4Ti_{21}O_{48}$, showed monoclinic symmetry, with possible space groups Cm, $C2$ or $C2/m$ and with approximate cell parameters $a=51{\cdot}0$, $b=2{\cdot}97$, $c=10{\cdot}30$ Å, $\beta=103{\cdot}20°$. This tabular crystal $0{\cdot}10\times1{\cdot}15\times0{\cdot}05$ mm was mounted along **b** on a Philips PW1100 four-circle automatic diffractometer. Nineteen high-angle reflexions provided the 2θ values used to calculate the lattice parameters reported in Table 1.

Table 1. *Crystallographic data for* $Ga_4Ti_{21}O_{48}$

Monoclinic		
a = 51·80 (2) Å	Formula weight	2052·8
b = 2·975 (1)	Density (calc.)	4·42 g cm^{-3}
c = 10·302 (4)	Systematic extinctions	hkl, $h+k\neq2n$
β = 103·80 (2)°	Space group	$C2/m$
Z = 2		

For the intensity data collection, special care was taken in selecting suitable slit conditions to eliminate interference from the minor superstructure reflexions. A series of manual scans through different superlattice reflexions showed that unresolvable overlap of reflexions from the two superstructures only occurred for singlets and doublets centred at the subcell positions.

Intensities were collected with graphite monochromated Mo $K\alpha$ radiation with a take-off angle of 12·18° and with a detector aperture of $1{\cdot}0\times1{\cdot}0°$. A θ–2θ scan (3–25°) was used with a variable scan width given by $\Delta\theta=(1{\cdot}00+0{\cdot}3\tan\theta)°$ and a speed of 0·05° s^{-1}. Two background measurements, each for half the scan time, were made for each scan, one at the lower and one at the upper limit. A total of 1656 independent reflexions were measured of which 1046 having $F^2>3\sigma(F^2)$ were used in the subsequent refinement.

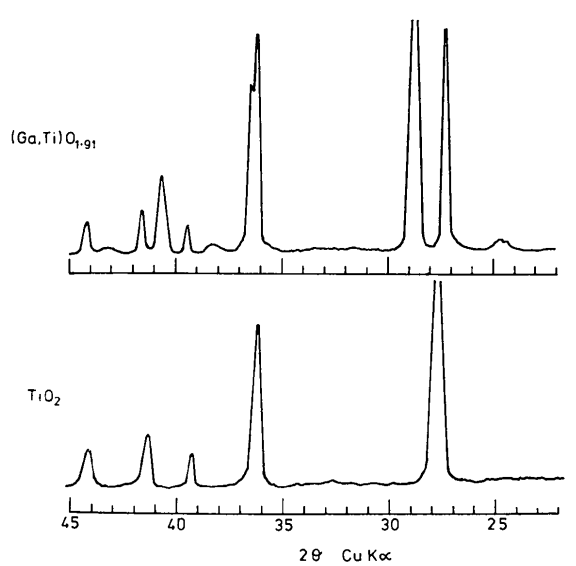

Fig. 1. Powder X-ray diffractograms, Cu $K\alpha$ radiation, for rutile and $Ga_4Ti_{21}O_{48}$.

Intensity data were processed by use of a program written for the PW1100 diffractometer (Hornstra & Stubbe, 1972). The background-corrected intensities were assigned standard deviations according to: $\sigma(I)=[CT+(t_c/t_b)^2(B_1+B_2)+(pI)^2]^{1/2}$ where CT is the total integrated peak count obtained in a scan time t_c; B_1 and B_2 are background counts each obtained in time $\frac{1}{2}t_b$, and $I=CT-(t_c/t_b)(B_1+B_2)$; p was 0·04. The inclusion of this last term is to allow for 'machine errors'. Values of I and $\sigma(I)$ were then corrected for Lorentz and polarization effects. Neither extinction nor absorption corrections were applied.

Scattering factor curves for Ga, Ti and O were obtained from Cromer & Waber's (1965) tabulation. All computing was performed on the Monash University CDC3200 and the CSIRO CDC7600 computers.

Electron microscopy

Samples were prepared for electron microscopy studies by grinding in chloroform and depositing the suspension on a holey carbon film. Thin edges, overlapping holes in the film, were examined at × 700 000 in a JEM-100C electron microscope.

Table 2. *Final atomic parameters for* $Ga_4Ti_{21}O_{48}$

	x	y	z	B(Å^2)
Ti(1)	0·0000	0	0·0000	0·13 (17)
Ti(2)	0·04084 (7)	0	0·45049 (35)	0·17 (12)
Ti(3)	0·08132 (7)	0	0·89893 (33)	0·04 (12)
Ti(4)	0·12180 (7)	0	0·34864 (34)	0·06 (12)
Ti(5)	0·16329 (7)	0	0·80063 (36)	0·21 (12)
Ti(6)	0·20280 (7)	0	0·25046 (35)	0·11 (12)
Ti(7)	0·35771 (7)	0	0·92577 (34)	0·08 (12)
Ti(8)	0·39793 (7)	0	0·37487 (34)	0·18 (12)
Ti(9)	0·43914 (7)	0	0·82610 (34)	0·11 (12)
Ti(10)	0·47979 (7)	0	0·27529 (33)	0·15 (12)
M(11)	0·27733 (5)	0	0·01578 (24)	0·25
(0·64Ga + 0·36Ti)				
M(12)	0·31766 (7)	0	0·47722 (33)	0·13
(0·09Ga + 0·91Ti)				
Ga	0·23753 (5)	0	0·70908 (22)	0·21 (7)
O(1)	0·06916 (23)	0	0·0675 (12)	−0·09 (45)
O(2)	0·05322 (24)	0	0·2821 (12)	0·29 (49)
O(3)	0·11029 (24)	0	0·5169 (12)	0·12 (47)
O(4)	0·02836 (22)	0	0·6185 (12)	−0·12 (45)
O(5)	0·09399 (22)	0	0·7319 (11)	−0·16 (45)
O(6)	0·01259 (24)	0	0·8317 (12)	0·17 (47)
O(7)	0·21546 (24)	0	0·0875 (12)	0·32 (49)
O(8)	0·13423 (24)	0	0·1810 (12)	0·18 (47)
O(9)	0·19191 (24)	0	0·4206 (12)	0·14 (48)
O(10)	0·17516 (25)	0	0·6313 (12)	0·24 (48)
O(11)	0·23805 (24)	0	0·8919 (12)	−0·13 (45)
O(12)	0·15097 (24)	0	0·9682 (12)	0·19 (48)
O(13)	0·31240 (24)	0	0·1365 (12)	0·16 (47)
O(14)	0·36052 (24)	0	0·2677 (12)	0·13 (47)
O(15)	0·28013 (25)	0	0·3664 (12)	0·22 (49)
O(16)	0·35400 (24)	0	0·5840 (12)	0·06 (46)
O(17)	0·27166 (23)	0	0·6867 (12)	−0·10 (46)
O(18)	0·32071 (23)	0	0·8146 (12)	−0·04 (46)
O(19)	0·39464 (24)	0	0·0348 (12)	−0·02 (46)
O(20)	0·44229 (23)	0	0·1699 (12)	−0·12 (46)
O(21)	0·43516 (24)	0	0·4825 (12)	0·01 (46)
O(22)	0·48318 (24)	0	0·6171 (12)	0·08 (46)
O(23)	0·40183 (23)	0	0·7188 (12)	−0·04 (46)
O(24)	0·47591 (24)	0	0·9319 (12)	−0·19 (47)

Structure determination and refinement

A three-dimensional Patterson map was computed which showed clearly the presence of the rutile substructure. From this a trial model was calculated in $C2/m$ using 13 unique titanium atoms including one at the origin. The metal atom positions were refined and a difference Fourier calculated which revealed all oxygen atoms (24) and indicated that two of the metal atom sites, which were initially given a titanium scattering curve, required extra electrons. These were assigned as gallium atoms. A structure factor calculation including all atoms gave R and wR of 0·237 and 0·276 respectively for all 1046 significant reflexions. $\{R=||F_o|-|F_c||/\sum|F_o|$ and $wR=[\sum w(|F_o|-|F_c|)^2/\sum w|F_o|^2]^{1/2}.\}$

After four cycles of block-diagonal least-squares refinement the positional and isotropic thermal parameters converged to give $R=0{\cdot}085$ and $wR=0{\cdot}101$. At this stage a study of the temperature factors suggested that one of the metal atom sites was fully occupied by gallium and two other sites contained major and minor fractions of gallium. The temperature factors for these two atoms were fixed at 0·25 and 0·13 which represented the refined B value for the fully occupied gallium site, and the average B for the titanium atoms respectively. In a further series of refinements these B values were kept constant and the multipliers for the two mixed atom sites were varied as well as all coordinates and thermal parameters. The resulting final R and wR values were 0·081 and 0·097. Removal of all the subcell reflexions, which were contributed to by the second phase, followed by refinement of all parameters, gave R and wR values of 0·85 and 0·097 for the remaining 845 reflexions.* No significant change in parameters resulted. The final positional and thermal parameters are given in Table 2. Bond lengths are given in Table 3.

* A list of structure factors has been deposited with the British Library Lending Division as Supplementary Publication No. SUP 31547 (3 pp.). Copies may be obtained through The Executive Secretary, International Union of Crystallography, 13 White Friars, Chester CH1 1NZ, England.

Table 3. *Selected bond lengths* (Å) *for* $Ga_4Ti_{21}O_{48}$

Standard deviations are about 0·018 Å for M–O and 0·025 Å for O–O.

Ti(1) Octahedron		Ti(2) Octahedron		Ti(3) Octahedron		Ti(4) Octahedron	
Ti(1)—O(24) (×4)	1·961	Ti(2) –O(21) (×2)	1·956	Ti(3) –O(20) (×2)	1·950	Ti(4) –O(23) (×2)	1·946
–O(6) (×2)	1·996	–O(22) (×2)	1·957	–O(19) (×2)	1·957	–O(16) (×2)	1·961
		–O(2)	1·989	–O(1)	1·982	–O(3)	1·966
		–O(4)	1·989	–O(5)	1·991	–O(8)	1·983
O(24) –O(24) (×2)	2·56	O(21)–O(22) (×2)	2·55	O(19)–O(20) (×2)	2·54	O(16)–O(23) (×2)	2·54
O(6) —O(24) (×4)	2·79	–O(2) (×2)	2·78	–O(5) (×2)	2·77	–O(8) (×2)	2·77
$O(6)^1$—O(24) (×4)	2·81	O(22)–O(4) (×2)	2·79	O(20)–O(5) (×2)	2·718	–O(3) (×2)	2·77
$O(24)^1$–O(24) (×2)	2·97	–O(2) (×2)	2·80	–O(1) (×2)	2·80	O(23)–O(3) (×2)	2·78
		O(21)–O(4) (×2)	2·80	O(19)–O(1) (×2)	2·80	–O(8) (×2)	2·78
		$O(22)–O(22)^1$ (×2)	2·97	$O(20)–O(20)^1$ (×2)	2·97	$O(16)–O(16)^1$ (×2)	2·97
Ti(5) Octahedron		**Ti(6) Octahedron**		**Ti(7) Octahedron**		**Ti(8) Octahedron**	
Ti(5) –O(14) (×2)	1·955	Ti(6) –O(18) (×2)	1·937	Ti(7) –O(8) (×2)	1·954	Ti(8)–O(5) (×2)	1·950
–O(13) (×2)	1·958	–O(7)	1·942	–O(12) (×2)	1·960	–O(3) (×2)	1·965
–O(12)	0·979	–O(9)	1·963	–O(14)	1·985	–O(21)	1·996
–O(10)	1·981	–O(17) (×2)	1·994	–O(18)	2·000	–O(14)	2·002
O(13)–O(14) (×2)	2·54	O(17)–O(18) (×2)	2·57	O(8)—O(12) (×2)	2·55	O(5)–O(3) (×2)	2·55
–O(10) (×2)	2·75	–O(7) (×2)	2·71	–O(18) (×2)	2·77	–O(21) (×2)	2·79
O(14)–O(10) (×2)	2·77	O(18)–O(7) (×2)	2·77	O(12)–O(18) (×2)	2·80	–O(14) (×2)	2·80
–O(12) (×2)	2·79	–O(9) (×2)	2·78	O(19)–O(8) (×2)	2·80	O(3)–O(21) (×2)	2·80
O(13)–O(12) (×2)	2·82	O(17)–O(9) (×2)	2·83	–O(12) (×2)	2·80	–O(14) (×2)	2·80
$–O(13)^1$ (×2)	2·97	–O(17) (×2)	2·97	O(8)—O(8) (×2)	2·97	O(5)–O(5) (×2)	2·97
Ti(9) Octahedron		**Ti(10) Octahedron**		**M(11) Octahedron**		**M(12) Octahedron**	
Ti(9)–O(2) (×2)	1·954	Ti(10)–O(6) (×2)	1·946	M(11)–O(7) (×2)	1·918	M(12)–O(10) (×2)	1·951
–O(1) (×2)	1·956	–O(4) (×2)	1·951	–O(13)	1·951	–O(9) (×2)	1·954
–O(24)	1·971	–O(22)	1·987	–O(11) (×2)	2·029	–O(16)	1·958
–O(23)	1·998	–O(20)	2·000	$–O(11)^1$	2·134	–O(15)	2·018
O(2)–O(1) (×2)	2·54	O(4)—O(6) (×2)	2·52	O(11)–O(7) (×2)	2·57	O(10)–O(9) (×2)	2·53
–O(23) (×2)	2·78	–O(20) (×2)	2·77	$–O(11)^1$ (×2)	2·71	–O(15) (×2)	2·76
O(1)–O(24) (×2)	2·78	O(6)—O(20) (×2)	2·79	$–O(7)^1$ (×2)	2·81	O(9)—O(15) (×2)	2·76
–O(23) (×2)	2·79	O(4)—O(22) (×2)	2·79	O(7)—O(13) (×2)	2·84	O(16)–O(10) (×2)	2·81
O(2)–O(24) (×2)	2·79	O(6)—O(22) (×2)	2·80	$–O(7)^1$ (×2)	2·97	–O(9) (×2)	2·81
$O(1)–O(1)^1$ (×2)	2·97	$–O(6)^1$ (×2)	2·97	O(13)–O(11) (×2)	2·97	O(10)–O(10) (×2)	2·97

Ga Tetrahedron			
Ga–O(15) (×2)	1·818	$O(15)–O(15)^1$	2·97
–O(17)	1·849	–O(11) (×2)	2·99
–O(11)	1·880	–O(17) (×2)	3·01
		O(17)–O(11)	2·05

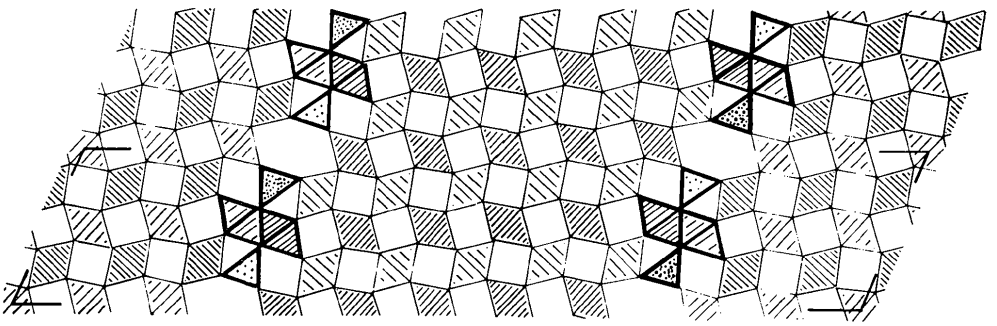

(*a*)

Fig. 2. (*a*) 3 Å projection for $Ga_4Ti_{21}O_{48}$. β-Gallia heavily outlined. Shading of polyhedra indicates two levels.

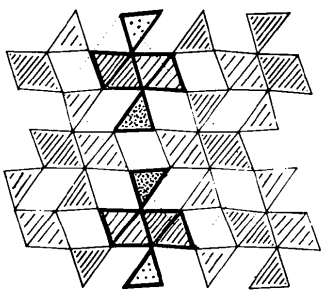

(*b*)

Fig. 2 (*cont.*). (*b*) 3 Å projection of β-Ga_2O_3 (Geller, 1960). β-Gallia elements heavily outlined. Shading of polyhedra indicates two levels.

Description of the structure

The structure of $Ga_4Ti_{21}O_{48}$ is shown in projection down the 3 Å axis (*i.e.* c_r) in Fig. 2(*a*). The two metal atom sites which together contain over 80% of the gallium have their coordination polyhedra heavily outlined. For comparison, the structure of β-Ga_2O_3 (Geller, 1960) in the same projection is shown in Fig. 2(*b*). It is clear that $Ga_4Ti_{21}O_{48}$ is a coherent intergrowth, parallel to $(210)_r$, of rutile structure and β-Ga_2O_3 structure elements. In the β-gallia structure gallium atoms occupy both tetrahedral and octahedral sites. The octahedra link pair-wise by edge-sharing which further articulate to give double chains of edge-shared octahedra parallel to the 3 Å axis. The double chains share corners with parallel strings of corner-shared tetrahedra to give the columnar structure shown heavily outlined in Fig. 2(*b*). As seen in Fig. 2(*a*), these columns of β-Ga_2O_3 occur as structure elements in $Ga_4Ti_{21}O_{48}$. However the disposition of adjacent columns differs in the two structures. In Fig. 2(*b*) it is necessary to rotate alternate columns by 180° about *A*, then repel them slightly to generate the structure of the displacement boundaries of $Ga_4Ti_{21}O_{48}$, Fig. 2(*a*). The β-Ga_2O_3-like columns are separated by large tunnels of hexagonal outline, having a periodicity of 10·3 Å$=c$, and an effective diameter of 2·5 Å. An atom situated in the tunnels would have ninefold coordination to oxygens with M–O distances from about 2·3 to 2·8 Å. The anion arrangement about the displacement boundary is shown in the ball and spoke representation of Fig. 3. Across the $(210)_r$ displacement boundary, adjacent rutile blocks are displaced by $[\frac{1}{2}\frac{1}{4}\frac{1}{2}]_r$. In the rutile slabs the shape of the metal–oxygen octahedra is almost identical to that in rutile, with two long M–O bonds and four shorter bonds, *e.g.* M(1) has 2M–O of 1·99 Å and 4M–O of 1·96 Å, compared with 2Ti–O of 1·982 Å and 4Ti–O of 1·946 Å in rutile (Cromer & Herrington, 1954). The average of the mean M–O distances for all metals in the rutile blocks, 1·965, is slightly longer than that for rutile, 1·958 Å, indicating some distribution of gallium into these sites. Within the β-gallia-like columns, the tetrahedral site, which is fully occupied by gallium, has a very regular angular arrangement of anions, with O–Ga–O angles in the narrow range 108·1 to 110·5°, although the bond lengths are irregular, ranging from 1·82 to 1·88 Å. The average Ga–O distance of 1·84 Å compares well with the value of 1·83 Å in β-Ga_2O_3. The octahedral site in the double edge-shared chains is very distorted, with O–M–O angles ranging from 81·1° to 101·5°, and with M–O bond lengths between 1·92 Å and 2·13 Å. The mean M–O length of 1·99 Å agrees with the value of 1·985 Å, calculated from the ionic radii for (0·64Ga + 0·36Ti)–O (Shannon & Prewitt, 1969). Along the direction of the chains, the M–M separation across the shared edge is constrained to the *b* axial length, 2·97 Å. However, for octahedra in adjacent chains, there is a considerable repulsion across the shared edge, with M–M = 3·22 Å.

Finally it is worth noting that the wavy layers of $(100)_r$ close packed oxygen layers in the rutile slabs are interrupted at the displacement boundary, where there occur segments of cubic close packed anion layers. However the c.c.p. is not continuous in the direction of the boundary, but broken by the anion layer displacements on the edges of the tunnels.

Discussion

The structural model for $Ga_4Ti_{21}O_{48}$, and other members of the homologous series $Ga_4Ti_{m-4}O_{2m-2}$, is quite different from that proposed by Gibb & Anderson (1972). This is understandable, as their model was constructed using an incorrect displacement vector, $[0\frac{1}{2}0]_r$, which is twice the length of the true displacement vector found in our studies, $[\frac{1}{2}\frac{1}{4}\frac{1}{2}]_r$ (see also Bursill & Stone, 1975). It is worth noting that Hyde, Bagshaw, Anderson & O'Keefe (1974) have previously suggested the possibility of incorporation of β-Ga_2O_3 elements into rutile as forming the structural basis for the $(210)_r$ structures. However because they considered possible structures in the light of Gibb & Anderson's incorrect displacement vector, they were unable to generate a satisfactory structural model.

The structure found for the (210) boundaries in $Ga_4Ti_{21}O_{48}$ corresponds to a true α-boundary. Indeed, the members of the homologous series may be described as rutile crystallographic shear, *CS*, structures; they may *formally* be described as derived from rutile by the periodic removal of a $(210)_r$ plane of atoms, followed by displacement of the rutile blocks by the vector $[-\frac{1}{2}\frac{1}{4}\frac{1}{2}]_r$. The *CS* operation is thus $[-\frac{1}{2}\frac{1}{4}\frac{1}{2}]_r(210)_r$. The operation is formally completed by very *minor* movements of metal and oxygen atoms at the boundary, resulting in half the metal atoms becoming tetrahedrally coordinated to oxygens. In the rutile structure, two types of atomic layers parallel to $(210)_r$ alternate, with compositions MO_4 and M. If we periodically remove every nth MO_4 layer, and follow the above *CS* operation, the composition of the *CS* phase is $M_{2n-1}O_{4n-4}$. For $n=13$ we have $M_{25}O_{48}$ corresponding to $Ga_4Ti_{21}O_{48}$. The next homologue in the series, with

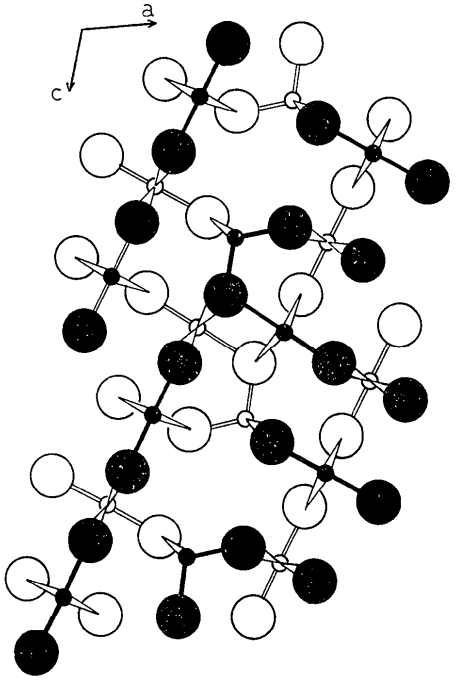

Fig. 3. A ball and spoke representation of the $(210)_r$ *CS* boundary in $Ga_4Ti_{n-4}O_{2n-2}$, viewed along **b**. Open circles represent atoms at $y=\frac{1}{2}$ and filled circles $y=0$.

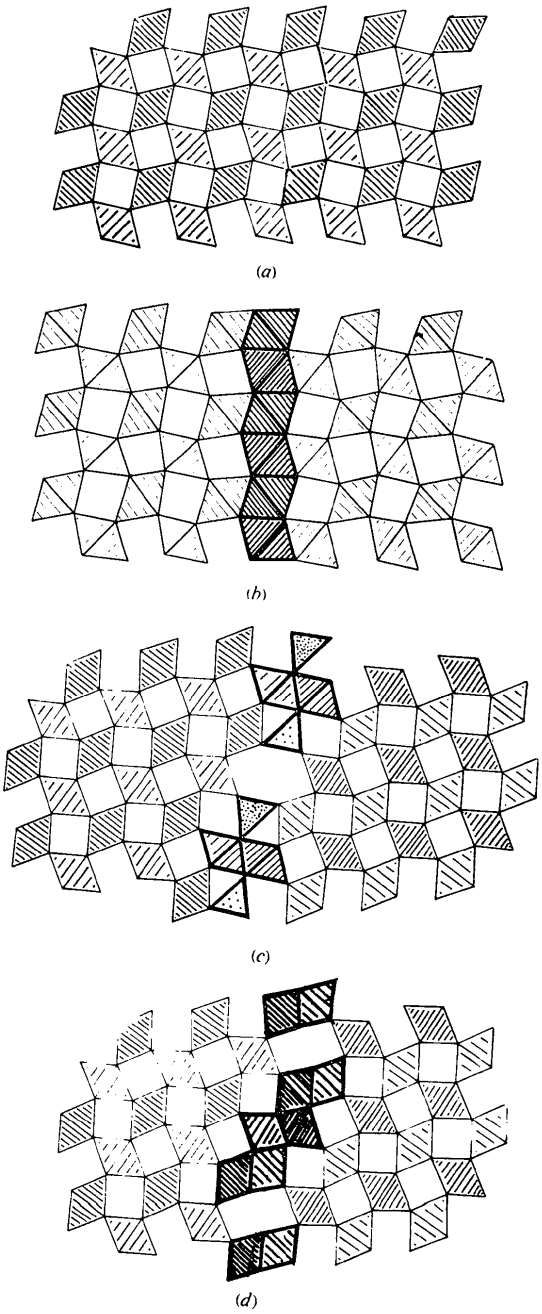

Fig. 4. (*a*) [001] projection of the rutile structure. (*b*) $[001]_r$ projection of a $(200)_r$ $[\frac{1}{2}0\frac{1}{2}]_r$ *CS* plane. This boundary may be regarded as an intergrowth of NiAs-type structure with rutile. In fact it is defective NiAs-type with metal occupancy of ~0·7 in the octahedral sites. (*c*) $[001]_r$ projecion of a $(210)_r$ $[\frac{1}{2}\frac{1}{4}\frac{1}{2}]_r$ boundary. β-gallia elements are heavily-lined. (*d*) $[001]_r$ projection of a $(211)_r$ $[\frac{1}{2}0\frac{1}{2}]_r$ boundary, showing elements of corundum-type structure intergrown with rutile. Only two $(001)_r$ layers are shown.

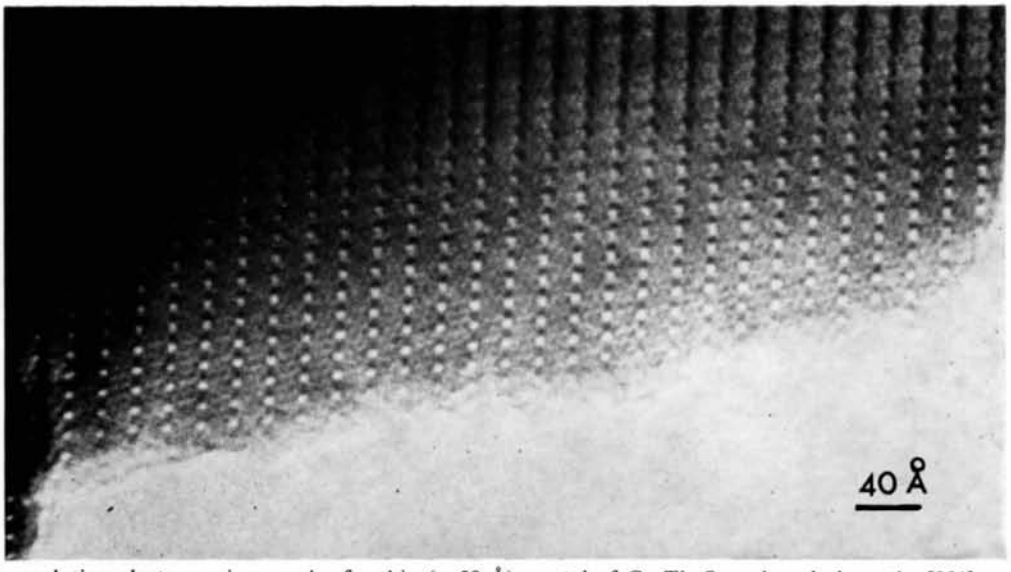

Fig. 5. High-resolution electron micrograph of a thin (~50 Å) crystal of $Ga_4Ti_{19}O_{36}$, viewed along the $[001]_r$ zone. There is a one-to-one correspondence between the white blobs and the position of the tunnels in the structure.

[*To face p.* 1761

$n=12$, $M_{23}O_{44}$, corresponds to $Ga_4Ti_{19}O_{44}$, *i.e.* if we use Gibb & Anderson's (1972) generic formula $Ga_4Ti_{m-4}O_{2m-2}$, then only odd values of m are possible, in accord with their observations. The above is a formalistic description of the relationship of the $(210)_r$ *CS* structure to that of rutile and is unsatisfactory in that it does not convey a mechanism for introducing the gallia into the rutile structure. Chemically, it would appear preferable to use the vector $[\frac{1}{2}\frac{1}{4}\frac{1}{2}]$ (which opens up a volume of thickness $\frac{5}{4}d_{210}$) and insert a slab of stoichiometric Ga_4O_6. The determination of the direction of the displacement vector requires an analysis of the Burgers vector at an isolated $(210)_r$ *CS* plane terminating within the rutile structure.

The series $Ga_4Ti_{m-4}O_{2m-2}$ represents the first known example of a rutile *CS* family in which the anion lattice is modified to cubic close packing at the *CS* plane. In the parent rutile structure, the anion arrangement is neither h.c.p. nor c.c.p. but forms wavy layers as shown in Fig. 4(*a*). For the $(121)_r$–$(132)_r$ rutile *CS* series in the binary system and the ternary Cr_2O_3–TiO_2 system (Bursill & Hyde, 1972) the anion lattice is modified to h.c.p. at the *CS* planes and the structures contain elements of hexagonal corundum structure, with face- and edge-shared chains of octahedra parallel to $[1\bar{1}1]_r$, Fig. 4(*d*). In the Fe_2O_3–TiO_2 system at high temperatures $(200)_r\frac{1}{2}[101]$ *CS* structures form which have complete planes of deficient NiAs structure type, parallel to $(100)_r$ (Bursill, Grey & Lloyd, 1976). The structure at the boundary for one of these phases is shown in Fig. 4(*b*), showing the flattening of the wavy rutile anion layers at the *CS* plane. Thus it appears that the rutile lattice can topologically deform to either h.c.p. or c.c.p., depending on the nature of the trivalent ion present and the O/M ratio, as well as other factors. It is remarkable that (211) $[\frac{1}{2}0\frac{1}{2}]$, (210) $[\frac{1}{2}\frac{1}{4}\frac{1}{2}]$ and (200) $[\frac{1}{2}0\frac{1}{2}]$ *CS* structures consist of a rutile matrix coherently intergrown with elements of the corundum, β-gallia and nickel arsenide-type structures respectively [Fig. 4(*a*)–(*d*)].

The gallium titanates, $Ga_4Ti_{m-4}O_{2m-2}$ are interesting in that they are the first examples of rutile *CS* structures in which the trivalent ion is proved to be ordered into the *CS* plane. The only other reported studies on ordering in rutile *CS* structures are for the Ti_nO_{2n-1} $(121)_r$ *CS* phases. Marezio, Dernier, McWhan & Kachi (1974) found that at room temperature Ti_4O_7 had a statistical distribution of Ti^{3+} and Ti^{4+} over all occupied metal sites while at lower temperatures, in the magnetically ordered state, the Ti^{3+} ions are ordered half into the *CS* plane and half in the rutile block.

We have found that both Cr^{3+} (at least 20 at.%) and Fe^{3+} (at least 40 at.%) will replace Ga^{3+} in the $(210)_r$ *CS* phases. Whereas Cr^{3+} will only substitute at octahedral sites, Fe^{3+} could replace Ga^{3+} both in the octahedral and tetrahedral sites.

Another possibility for compositional variation in the $(210)_r$ *CS* structures is for charged or uncharged species to occupy sites in the large tunnels. From the size of the tunnels, one could expect ions as large as Ca^{2+}, Pb^{2+} or Na^+ or molecules such as water to be stabilized in the structure. In the case of positive ions, charge balance could be achieved by replacement of some Ti^{4+} by a lower valence species, *e.g.* Cr^{3+} or Mg^{2+}. However, in the pure Ga_2O_3–TiO_2 system, these tunnels are empty. Because they are directed along the short *b* axis, 2·97 Å, the possibility existed for direct imaging by electron microscopy. A preliminary high-resolution microscopy study has verified this as shown in Fig. 5. In further studies we plan to apply the direct imaging technique to study the effect of ordering metal ions into the tunnels, and the mechanism of formation of the structures in a rutile matrix.

References

BURSILL, L. A., GREY, I. E. & LLOYD, D. J. (1976). *J. Solid State Chem.* In the press.

BURSILL, L. A. & HYDE, B. G. (1972). *Progr. Solid State Chem.* **7**, 177–253.

BURSILL, L. A. & STONE, G. G. (1975). *Phil. Mag.* **32**, 1151.

CROMER, D. T. & HERRINGTON, K. (1954). *J. Amer. Chem. Soc.* 77, 4708–4709.

CROMER, D. T. & WABER, J. T. (1965). *Acta Cryst.* **18**, 104–109.

GELLER, S. (1960). *J. Chem. Phys.* **33**, 676–684.

GIBB, R. M. & ANDERSON, J. S. (1972). *J. Solid State Chem.* **5**, 212–225.

HORNSTRA, J. & STUBBE, B. (1972). PW 1100 data processing program, Philips Research Labs., Eindhoven.

HYDE, B. G., BAGSHAW, A. N., ANDERSON, S. & O'KEEFE, M. (1974). *Ann. Rev. Mater. Sci.* **4**, 43–92.

MAREZIO, M., DERNIER, P. D., MCWHAN, D. B. & KACHI, S. (1974). *J. Solid State Chem.* **11**, 301–313.

SHANNON, R. D. & PREWITT, C. T. (1969). *Acta Cryst.* B**25**, 925–946.